Multi-pomeron repulsion and the Neutron-star mass

Y. Yamamoto[1], T. Furumoto[2], N. Yasutake[3], and Th.A. Rijken[41]

[1]*Nishina Center for Accelerator-Based Science, Institute for Physical and Chemical Research (RIKEN), Wako, Saitama, 351-0198, Japan*
[1]*Ichinoseki National College of Technology, Ichinoseki, Iwate, 021-8511, Japan*
[3]*Department of Physics, Chiba Institute of Technology, 2-1-1 Shibazono Narashino, Chiba 275-0023, Japan*
[4]*IMAPP, University of Nijmegen, Nijmegen, The Netherlands*

A multi-pomeron exchange potential (MPP) is proposed as a model for the three-body repulsion indicated in neutron-star matter, which works universally among three- and four-baryons. Its strength is determined by analyzing the nucleus-nucleus scattering with the G-matrix folding model. The EoS in neutron matter is obtained including the MPP contribution. The neutron-star mass is calculated by solving the TOV equation. The maximum mass is obtained to be larger than the observed one $1.97 M_{solar}$ on the basis of the experimental data.

I. INTRODUCTION

The new observation of the system J1614-2230 [1] has brought a great impact on the maximum-mass problem of neutron stars. The large observed value of neutron-star mass $1.97 M_{solar}$ gives a severe condition for the stiffness of the equation of state (EoS) of neutron-star matter.

For realization of the nuclear saturation property based on underlying nuclear interactions, an essential role is played by the three-nucleon (N) interaction (TNI) composed of the attractive part (TNA) and the repulsive part (TNR). Especially, the TNR contribution increasing rapidly in the high-density region leads to a high values of nuclear incompressibility: The TNR contribution in high-density neutron matter plays an essential role for stiffening of the EoS of neutron-star matter, assuring the observed maximum mass of neutron stars.

However, the hyperon (Y) mixing in neutron-star matter brings about the remarkable softening of the EoS, which cancels the TNR effect for the maximum mass. In order to avoid this serious problem, Nishizaki, Takatsuka and one of the authors (Y.Y.) [2] introduced the conjecture that the TNR-type repulsions work universally for YN and YY as well as for NN. They showed that the role of the TNR for stiffening the EoS can be recovered clearly by this assumption. Our basic concern is the existence of universal repulsions among three baryons, called here as the three-baryon repulsion (TBR).

In modeling for YN and YY interactions, important development has been accomplished by the Extended Soft Core (ESC) models. Here, two-meson and meson-pair exchanges are taken into account explicitly and no effective boson is included differently from the usual one-boson exchange models. The latest version of ESC model is named as ESC08c [3, 4]. Hereafter, ESC means this version. In this work, TBR is taken into account by the multi-pomeron exchange potential (MPP) within the ESC modeling. In order to reproduce the nuclear saturation property precisely, it is necessary to introduce also TNA. We treat this part phenomenologically.

The G-matrix theory gives a good starting point for studies of many-body systems on the basis of free-space baryon-baryon interaction models. Here, the correlations induced by short-range and tensor components are renormalized into G-matrix interactions. In the case of nucleon matter, the lowest-order G-matrix calculations with the continuous (CON) choice for intermediate single particle potentials were shown to simulate well the results including higher hole-line contributions up to $3 \sim 4$ times of normal density ρ_0 [5]. On the basis of this recognition, one can study properties of high-density nuclear matter using the lowest-order G-matrix theory with the CON choice.

One of great successes of the G-matrix approach is that nucleon-nucleus and nucleus-nucleus scattering observables are nicely reproduced with the complex G-matrix folding potentials derived from free-space NN interactions. In ref.[6], it was shown clearly that the TNR effect appeared in angular distributions of $^{16}O+^{16}O$ elastic scattering (E/A=70 MeV), *etc.* Their analysis is used here to determine the coupling constants in MPP: The G-matrix folding potentials including MPP contributions are used to analyze the $^{16}O+^{16}O$ scattering, and then the strengths of MPP are adjusted so as to reproduce the experimental data.

Many attempts have been made to extract some information on the incompressibility K of high-density matter formed in high-energy central heavy-ion collisions. In many cases, however, the results for the EoS still remain inconclusive. On the other hand, it was pointed out that folding-model analyses of high-precision nuclear scattering data can be used as an independent method to determine the value of K, which was demonstrated with use of density-dependent interactions [7, 8]. Our approach can be considered as a development from theirs: The MPP contributions determined by analyses with the G-matrix folding model are included in constructing the EoS of neutron-star matter, which is expected to result in a stiff EoS, enough to give the observed neutron-star mass.

The important feature of our MPP is that it works

universally not only in *NNN* states but also *YNN*, *YYN* and *YYY* states. It will be shown in our future work that inclusions of MPP's in hypernuclear calculations lead to reasonable results.

II. MULTI-POMERON POTENTIAL

We introduce the universal TBR consistently with the ESC modeling, assuming that the dominant mechanism is triple and quartic pomeron exchange. For the N-tuple pomeron vertex generally, we take the Lagrangian

$$\mathcal{L}_N = g_P^{(N)} \mathcal{M}^{4-N} \sigma_P^N(x)/N! \qquad (1)$$

The N-body local potential by pomeron exchange is

$$V(\mathbf{x}'_1, ..., \mathbf{x}'_N; \mathbf{x}_1, ..., \mathbf{x}_N) \equiv V(\mathbf{x}_1, ..., \mathbf{x}_N)\, \Pi_{i=1}^N \delta(\mathbf{x}'_i - \mathbf{x}_i),$$

$$V(\mathbf{x}_1, ..., \mathbf{x}_N) = g_P^{(N)} g_P^N \left\{ \int \frac{d^3 k_i}{(2\pi)^3} e^{-i\mathbf{k}_i \cdot \mathbf{x}_i} \right\}$$

$$\times (2\pi)^3 \delta(\sum_{i=1}^N \mathbf{k}_i) \Pi_{i=1}^N \left[\exp\left(-\mathbf{k}_i^2\right) \right] \mathcal{M}^{4-3N}, \qquad (2)$$

where the (low-energy) pomeron propagator is the same as used in the two-body pomeron potential. Since the pomeron is an SU(3)-singlet, MPP's work universally among baryons.

The effective two-body potential in a baryonic medium is obtained by integrating over the coordinates $\mathbf{x}_3, ..., \mathbf{x}_N$. This gives

$$V_{eff}^{(N)}(\mathbf{x}_1, \mathbf{x}_2) = \rho_{NM}^{N-2} \int d^3 x_3 ... \int d^3 x_N \ V(\mathbf{x}_1, \mathbf{x}_2, ..., \mathbf{x}_N)$$

$$= g_P^{(N)} g_P^N \frac{\rho_{NM}^{N-2}}{\mathcal{M}^{3N-4}} \frac{1}{\pi\sqrt{\pi}} \left(\frac{m_P}{\sqrt{2}}\right)^3 \exp\left(-\frac{1}{2} m_P^2 r_{12}^2\right), (3)$$

ρ_{NM} being a nuclear-matter density. We restrict ourselves here to the triple and quartic pomeron couplings.

Values of MPP strengths $g_P^{(3)}$ can be estimated from the experimental cross sections of the process $pp \to pX$ (diffractive production of showers of particles) at very high energies [9]: The estimated values are $g_P^{(3)}/g_P = 0.15 \sim 0.20$. Using the value of $g_P = 3.67$ used in ESC, we have

$$g_P^{(3)} = 1.95 \sim 2.6 \ .$$

In the Reggeon field theory [10], the value of $g_P^{(4)}$ can be estimated as

$$g_P^{(4)} = (8.8 \sim 60)\,(g_P^{(3)})^2 = 33 \sim 228 \ .$$

III. MPP IN NUCLEUS-NUCLEUS SCATTERING

In [6] the complex G-matrix interaction was derived from the ESC model including TNR, and nucleus-nucleus elastic scatterings were analyzed with the use of double-folding potentials. In this work, the TNR effect was assumed to come from the medium effect on the vector-meson masses differently from the present MPP model. When a scattering energy is high enough, the frozen-density approximation gives a good prescription. In this approximation, G-matrices at about two times of normal density contribute to folding potentials. Then, the TNR effects were shown to appear clearly in angular distributions in the case of ^{16}O+^{16}O elastic scattering at $E/A = 70$ MeV, and also in the cases of ^{16}O elastic scattering by the ^{12}C, ^{28}Si and ^{40}Ca at $E/A = 93.9$ MeV, and ^{12}C+^{12}C elastic scattering at $E/A = 135$ MeV. Here, the same analyses are performed so that the MPP strengths $g_P^{(3)}$ and $g_P^{(4)}$ are determined to reproduce the experimental data with the use of the G-matrix folding potential derived from ESC including MPP.

On the other hand, the nuclear saturation property cannot be reproduced only by adding MPP to ESC. Then, we introduce also a TNA part phenomenologically as a density-dependent two-body interaction

$$V_{TNA}(r; \rho) = V_{TNA}^0 \exp(-(r/2.0)^2)\, \rho \, \exp(-4.0\rho) \ . \quad (4)$$

Here, because the functional form is not determined within our analysis, it is fixed to be similar to the TNA part given in [12]. Only the strength V_{TNA}^0 is treated as an adjustable parameter.

This TNA is assumed to work only in even states: An odd-state TNA contributes to the ^{16}O+^{16}O potential at $E/A = 70$ MeV more than the nuclear-matter energy, because G-matrices in the former are with higher momenta than those in the latter. Therefore, they cannot be reproduced consistently, for instance, with use of a Wigner-type TNA. Also the Fujita-Miyazawa TNA used in [6] is specified by dominant contributions from even-state components.

On the basis of G-matrix calculations, strengths of the TNR part ($g_P^{(3)}$ and $g_P^{(4)}$) and the TNA part (V_{TNA}^0) are determined so as to reproduce the ^{16}O+^{16}O angular distribution $E/A = 70$ MeV and the minimum value ~ -16 MeV of the energy per nucleon at normal density in symmetric matter. Because the ratio of $g_P^{(3)}$ and $g_P^{(4)}$ cannot be determined in our analysis, it is taken adequately referring the above estimation based on [9, 10]. Then, we have $(g_P^{(3)}, g_P^{(4)})$= (2.34, 30.0) and $V_{TNA}^0 = -36$ MeV. This set is called as MP1a. In order to see a role of $g_P^{(4)}$ especially in high-density region, we take here another set $(g_P^{(3)}, g_P^{(4)})$= (2.94, 0.0) with the same value of V_{TNA}^0. This set without $g_P^{(4)}$ is called MP2a.

In Fig.1, the calculated results of the differential cross sections for the ^{16}O+^{16}O elastic scattering at $E/A = 70$ MeV are compared with the experimental data [11]. Here, the dotted curve is obtained with the G-matrix folding potential derived from MP0 meaning ESC without MPP, which deviates substantially from the data. Solid and dashed curves are for MP1a and MP2a, respectively, which are found to fit the data nicely. Though
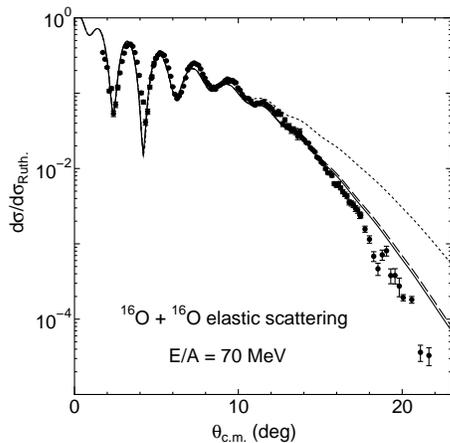
FIG. 1: Differential cross sections for ^{16}O+^{16}O elastic scattering at $E/A = 70$ MeV calculated with the G-matrix folding potentials. Solid and dashed curves are for MP1a and MP2a, respectively. Dotted curve is for MP0.

reduction factors are often multiplied on the imaginary parts in the folding model analyses [6], such a reduction factor is not used in the present analysis. The necessity to include the quartic pomeron coupling has to appear in the difference between results for MP1a and MP2a, but it cannot be found in the present analyses for nucleus-nucleus scattering.

IV. EQUATION OF STATE

In Fig.2, energies per nucleon in symmetric nuclear matter are drawn as a function of nucleon density ρ_N. The box in the figure show the area where nuclear saturation is expected to occur empirically. The dotted curve is obtained for MP0. Then, the saturation density and the minimum energy in symmetric matter are found to be deviated substantially from the box. Solid and dashed curves are for MP1a and MP2a, respectively. As seen clearly, saturation densities and minimum values in these cases are close nicely to the empirical value shown by the box. Then, obtained values of incompressibility K are 280 MeV and 270 MeV at minimum point in the cases of including MP1a and MP2a, respectively. which are comparable to the empirical value 240 ± 20 MeV [13, 14].

In Fig.3, we show energy curves of neutron matter, namely binding energy per neutron as a function of neutron density ρ_n. Solid and dashed curves are for MP1a and MP2a, respectively. Dotted curve is for MP0. The difference between the energy curves for neutron matter and symmetric matter gives the symmetry energy $E_{sym}(\rho)$, and its slope parameter is defined by $L = 3\rho_0 \left[\frac{\partial E_{sym}(\rho)}{\partial \rho} \right]$. The values of E_{sym} at normal density are 32.5, 33.4 and 33.5 MeV in the cases of MP0, MP1a and MP2a, respectively, and the values of L are 71, 72 and 73 MeV correspondingly. These values are
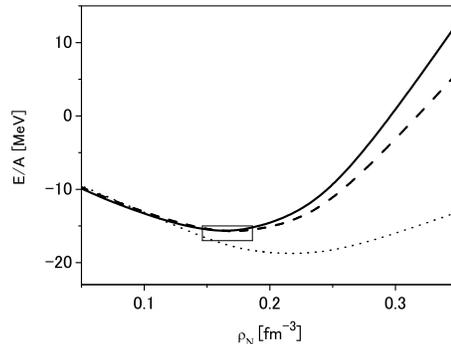
in nice agreement to the values $E_{sym} = 32.5 \pm 0.5$ MeV and $L = 70 \pm 15$ MeV determined recently on the basis of experimental data [15]. Thus, the nuclear saturation property derived from MP1a or MP2a is quite reasonable in comparison with the empirical values, as seen in obtained values of K, E_{sym} and L.
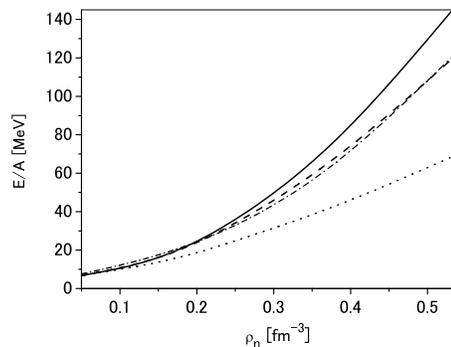

FIG. 2: Energy per particle of symmetric matter as a function of ρ_N. Solid and dashed curves are for MP1a and MP2a), respectively. Dotted curve is for MP0. The box shows the empirical value.

FIG. 3: Energy per particle of neutron matter as a function of ρ_n. Solid and dashed curves are for MP1a and MP2a, respectively. Dotted curve is for MP0. Dot-dashed curve is for UIX [16].

V. NEUTRON STAR MASS

Recently, the important roles of the three-neutron ($3n$) repulsion are studied for the EoS of neutron matter and the neutron-star mass [16]. Among their interactions, the stiffest EoS is given by the UIX model (the Argonne AV8' model combined with the Urbana IX). This EoS is stiff enough to explain the large neutron-star mass $1.97M_{solar}$ [1]. Their result for the UIX model is shown by the dot-dashed curve in Fig.3. Our results for MP1a (MP2a) turns out to be stiffer than (comparable to) theirs.

Using the EoS of pure neuron matter, we solve the Tolmann-Oppenheimer-Volkoff (TOV) equation for the

hydrostatic structure of a spherical non-rotating star, and obtain the mass and radius of neutron stars. From the G-matrix calculations, we obtain the energy per neutron as a function of density ρ. According to [16], the energy curve is parameterized as

$$E(\rho)/A = a \left(\frac{\rho}{\rho_0} \right)^\alpha + b \left(\frac{\rho}{\rho_0} \right)^\beta . \qquad (5)$$

The fitting parameters are given in Table I in the cases of MP0, MP1a and MP2a. These EoS's are used for $\rho > \rho_{crust} = \rho_0/10$. Below ρ_{crust} we use the EoS of the crust obtained in [17, 18].

TABLE I: Fitting parameters for the neutron matter EoS, a and b being in MeV.

	a	α	b	β
MP0	10.8	0.442	5.31	1.88
MP1a	11.4	0.481	7.70	2.41
MP2a	6.79	0.192	11.6	1.93

The EoS's for MP1a and MP2a violate causality and predict sound speeds over the speed of light above a critical density. Then, we adopt the approximation where the EoS is replaced by the causal EoS above this density in the same way as the treatment in [16].

In Fig.4 and Fig.5, the calculated star masses are given as a function of the radius R and the central density ρ_c, respectively. Solid and dashed curves are for MP1a and MP2a, respectively. Dotted curves are for MP0. The EoS's in the cases of including MPP contributions are found to be stiff enough to give maximum masses larger than the observed mass $M_{obs} = 1.97 M_{solar}$ for J1614-2230. The maximum masses for MP1a are substantially larger than that for MP2a. The difference is due to the quartic-pomeron exchange term included in the former. The strengths of the effective two-body interaction derived from triple- and quartic-pomeron exchanges are proportional to matter density ρ and ρ^2, respectively. Then, the contribution of the latter become sizeable in the high-density region, which makes the maximum mass large. However, the difference between MP1a and MP2a contributions cannot be seen in Fig.1, which means that the quartic-pomeron exchange contribution demonstrated in neutron-star masses cannot be found by analyses of nucleus-nucleus scattering data.

VI. CONCLUSION

In order to explain the observed maximum mass of neutron stars, three-body repulsions are considered to work universally among three baryons. The multi-pomeron potential (MPP) is introduced as a model for such a universal three-body repulsion. Furthermore, the three-nucleon attraction (TNA) is added phenomenologically so as to reproduce the nuclear saturation property precisely. The strengths of MPP and TNA can
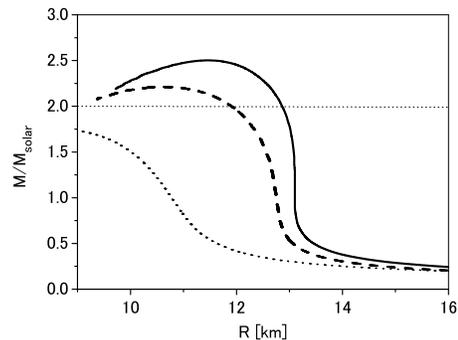

FIG. 4: Neutron-star masses as a function of the radius R. Solid and dashed curves are for MP1a and MP2a, respectively. Dotted curve is for MP0.
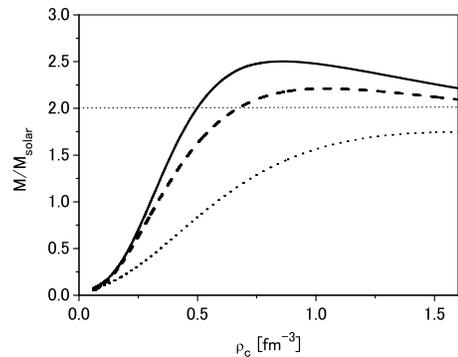

FIG. 5: Neutron-star masses as a function of the central density ρ_c. Also see the caption of Fig.4.

be determined by fitting the observed angular distribution of $^{16}O+^{16}O$ elastic scattering at $E/A = 70$ MeV with use of the G-matrix folding potential derived from ESC+MPP+TNA and adjusting to reproduce the minimum value ~ -16 MeV of the energy per nucleon at normal density in symmetric nuclear matter. Then, the empirical values of K, E_{sym} and L are reproduced reasonably. The EoS of neutron-star matter obtained from ESC+MPP+TNA is stiff enough to give the large neutron-star mass over $1.97 M_{solar}$. It should be noted that our stiff EoS is determined with use of the experimental data for nucleus-nucleus scattering and nuclear saturation properties. Our MPP contributions exist universally in every baryonic system. It is our future subject to show that our stiff EoS with universal MPP repulsions is free from the softening effect induced by hyperon mixing to neutron-star matter. Such a work will be complementary to the analyses based on the relativistic mean field models [19–21] for a massive neutron star including hyprons.

---

[1] P.B. Cemorest, T. Pennucci, S.M. Ransom, M.S.E. Roberts, and J.W. Hessels, Nature (London) **467**, 1081 (2010).

[2] S. Nishizaki, Y. Yamamoto, and T. Takatsuka, Prog. Theor. Phys. **105**, 607 (2001); **108**, 703 (2002).

[3] Th.A. Rijken, M.M. Nagels, and Y. Yamamoto, Prog. Theor. Phys. Suppl. **185**, 14 (2010).

[4] Th.A. Rijken, M.M. Nagels, and Y. Yamamoto, in *Proceedings of the International Workshop on Strangeness Nuclear Physics*, Neyagawa 2012, Genshikaku Kenkyu **57**, Suppl.3, 6 (2013).

[5] M. Baldo, A. Fiasconaro, H.Q. Song, G. Giansiracusa, and U. Lombardo, Phys. Rev. C**65**, 017303 (2001).

[6] T. Furumoto, Y. Sakuragi, and Y. Yamamoto, Phys. Rev. C**79**, 011601(R) (2009); C**80**, 044614 (2009).

[7] D.T. Khoa, et al., Phys. Rev. Lett. **74**, 34 (1995).

[8] D.T. Khoa, G.R. Satchler, and W.von Oertzen, Phys. Rev. C**56**, 954 (1997).

[9] A.B. Kaidalov and K.A. Ter-Materosyan, Nucl. Phys. **74**, 471 (1974).

[10] J.B. Bronzan and R.L. Sugar, Phys. Revs. D**16**, 466 (1977).

[11] F. Nuoffer, et al., Nuovo Cimento A**111**, 971 (1998).

[12] I.E. Lagaris and V.R. Pandharipande, Nucl. Phys. A**359**, 349 (1981).

[13] G. Colò, N. Van Giai, J. Meyer, K. Bennaceur, and P. Bonche, Phys. Rev. C**70**, 024307 (2004).

[14] Li-Gang Cao, H. Sagawa, and G. Colo, Phys. ReV. C**86**, 054313 (2012).

[15] P. Möller, W.D. Myers, H. Sagawa and S. Yoshida, Phys. Rev. Lett. **108**, 052501 (2012).

[16] S. Gandolfi, J. Carlson, and Sanjjay Reddy, Phys. Rev. C**85**, 032801(R) (2012).

[17] G. Baym, A. Bethe, and C. Pethick, Nucl. Phys. A**175**, 225 (1971).

[18] G. Baym, C.J. Pethick, and P. Sutherland, Astrophys. J.**170**, 299 (1971).

[19] S. Weissenborn, D. Chatterjee, and J. Schaffner-Bielich, Nucl. Phys. A**881**, 62 (2012).

[20] I. Bednarek, P. Haensel, J.L. Zdunik, M. Bejger, and R. Manka, Astronomy & Astrophysics A**157**, 543 (2012).

[21] Wei-Zhou Jiang, Bao-An Li, and Lie-Wen Chen, Astrophys. J.**756**, 56 (2012).